Accepted Manuscript

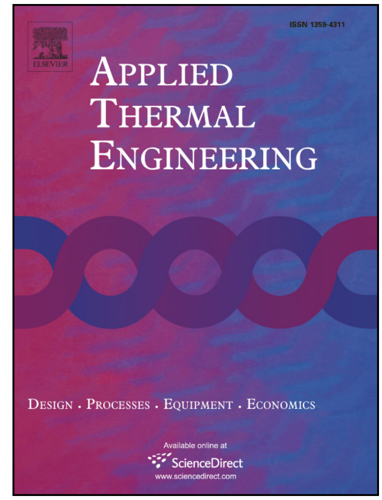

Steady state investigations of a commercial diffusion-absorption refrigerator: Experimental study and numerical simulations

Rami Mansouri, Mahmoud Bourouis, Ahmed Bellagi

PII: S1359-4311(16)34487-8
DOI: https://doi.org/10.1016/j.applthermaleng.2017.10.010
Reference: ATE 11208

To appear in: *Applied Thermal Engineering*

Received Date: 29 December 2016
Revised Date: 30 July 2017

Please cite this article as: R. Mansouri, M. Bourouis, A. Bellagi, Steady state investigations of a commercial diffusion-absorption refrigerator: Experimental study and numerical simulations, *Applied Thermal Engineering* (2017), doi: https://doi.org/10.1016/j.applthermaleng.2017.10.010

Steady state investigations of a commercial diffusion-absorption refrigerator: Experimental study and numerical simulations

Rami Mansouri[a,b], **Mahmoud Bourouis**[b*], **Ahmed Bellagi**[a]

[a]U. R. Thermique & Thermodynamique des Procédés Industriels
Ecole Nationale d'Ingénieurs de Monastir, ENIM
Avenue Ibn El Jazzar, 5019 Monastir
University of Monastir – Tunisia

[b]Department of Mechanical Engineering, Universitat Rovira i Virgili,
Av. PaïsosCatalans No. 26, 43007Tarragona, Spain

*Corresponding author
Email: mahmoud.bourouis@urv.cat

Abstract

Experimental investigations and numerical simulations of a low capacity commercial diffusion-absorption refrigerator (DAR) in stationary mode are carried out. The tests are performed under different heat input conditions. Optimal operation of the DAR refrigerator is reached with a power supply of 46 W at a generator temperature of 167ºC, corresponding to a coefficient of performance (COP) of 0.159. Numerical simulations of the refrigerator using a model developed with the commercial flow-sheeting Aspen-Plus software are also perfomed. The computer model is validated by comparing its predictions with experimental data for three generator heat supply rates: 46W, 56W and 67W. Deviations between model predictions and experimental measurements in terms of cooling capacity and coefficient of performance are less than 1%. The proposed model could be very useful to predict the functioning of the commercial diffusion-absorption refrigerator under steady-state regime.

Keywords: diffusion-absorption refrigeration, ammonia/water/hydrogen, steady-state mode, Aspen-Plus.

Highlights

- Experimental investigations of a commercial DAR refrigerator are carried out.
- A detailed steady-state simulation model of the DAR is developed using Aspen-Plus.
- The refrigerator model is validated using the experimental measurements.

Nomenclature

COP	Coefficient of performance (-)
$\dot{Q}_{gen}$	Generator heat supply (W)
$\dot{Q}_{heat}$	Electric cable heat supply (W)
$\dot{Q}_{evap}$	Cooling capacity (W)
R	Resistance of the electric cable (Ω)
T	Temperature (°C)
(UA)	Overall heat transfer coefficient (W K^{-1})
φ	Applied voltage (V)

Subscripts

amb	Ambient
cab	Refrigerated room cabinet
elec	Electric
evap	Evaporator
gen	Generator
int	Refrigerator interior
in	Evaporator input
out	Evaporator output

1. Introduction

Absorption refrigeration systems use natural fluid mixtures, such as ammonia/water (NH_3/H_2O), water/lithium bromide (H_2O/LiBr) and methanol/lithium bromide (CH_3OH/LiBr) as working pairs, instead of the harmful chloro-fluoro-carbon and chloro-hydro-fluoro-carbon (CFC/CHFC) fluids found in common vapour compression refrigeration and air conditioning systems. The idea of eliminating the pump circulating the solution and making the pressure uniform in all components of the absorption refrigeration systems occurred first to Geppert in 1899 [1]. To allow the refrigerant to evaporate at low temperatures in the evaporator, a third compound i.e. an inert gas was introduced. A diffusion-absorption refrigeration cycle or a pumpless vapour absorption refrigeration cycle is of great significance in noiseless refrigeration applications. The diffusion-absorption cycle is unique in that it runs without any mechanical energy input. This is achieved by pumping the working fluid using a thermally driven bubble pump. Another unique feature of this cycle is that it is essentially noise free. The first diffusion-absorption refrigeration (DAR) machine using this technique for cold production was developed by the Swedish engineers von Platen and Munters in 1928 [2]. In this refrigerator, ammonia was used as a refrigerant, water as an absorbent and hydrogen as an inert gas to equalize the pressure. Since the invention of the diffusion-absorption refrigeration systems, much research has been conducted in order to make them more attractive for use as domestic refrigerators and to improve their performance. Most of these investigations were focussed on improving the performance by reducing the heat supplied to the generator. Many aspects were then discussed, such as the mechanical design of the various components of these systems, the thermodynamic cycles and the nature of the working fluids. Kouremenos *et al*. [3] examined the possibility of using helium instead of hydrogen as the inert gas. They reported that this gas behaved in a similar manner to hydrogen. Chen *et al*. [4] improved the coefficient of performance of a DAR system by 50%, by modifying the design and construction of the generator and equipping it with a heat exchanger. Vicatos [5] carried out an experimental study of a domestic DAR system and modified it in order to reduce the response time of the system. Zohar *et al*. [6] developed a thermodynamic model of a DAR system and performed a parametric study that showed that the best performances would be obtained with an ammonia mass fraction of 30% for the rich solution and of 10% for the lean solution. They also found that the COP of an optimized system with helium as an inert gas was 40% higher than that of the conventional DAR system. Ben Ezzine *et al*. [7] investigated the feasibility of a DAR system operating with the working fluid mixture DMAC-R124-He for solar applications. They showed that the COP and the produced cold temperature depended largely on the effectiveness of the absorber and on the generator temperature and concluded that the considered fluid mixture might be an alternative to the conventional ammonia/water/hydrogen system. Sayadi *et al*. [8] presented a simulation model using the commercial flow-sheeting software HYSYS for a water-cooled DAR system using various binary mixtures of light hydrocarbons (C_3/*n*-C_6, C_3/cyclo-C_6, C_3/cyclo-C_5, propylene/cyclo-C_5, propylene/*i*-C_4, and propylene/*i*-C_5) as working fluids and helium as an inert gas. The heat input into the generator was assumed to be provided by evacuated tube solar collectors. The most appropriate binary fluid mixture was found to be (C_3/*n*-C_6) with a generator temperature of 126°C. Mazouz *et al*. [9] carried out an experimental study of a commercial DAR machine in order to determine its performance parameters under various operating conditions. Steady state and dynamic methods were applied to evaluate the characteristics of the machine. The best performance of the machine was obtained with a heat supply of 42W. A value of 0.12 was found for the COP.Narayankhedkar and Maita [10] showed the existence of an optimal power supply which yielded a maximum refrigerating effect, based on theoretical and experimental investigations of a diffusion-absorption refrigerator. Zohar *et al.* [11] presented a thermodynamic model for an ammonia/water/hydrogen DAR system and investigated two configurations of the diffusion-absorption cycle, namely those with and without a condensate sub-cooling prior to the evaporator entrance. They reported that the configuration without a condensate sub-cooling showed a higher COP by 14-20% for an evaporator temperature of 15°C. In reference [12], Zohar *et al.* examined the performance of a simplified DAR system with an organic absorbent (DMAC-dimethylacetamide) and five different refrigerants (R22, R32, R124, R125 and R134a) and helium as an inert gas. The comparison with the ammonia/water/helium DAR system showed that the latter achieved a higher COP (0.298) at a generator temperature of 150°C and an evaporator temperature of -18°C. Among the organic refrigerants, R22 provides the highest COP (0.224) at a generator temperature of 143°C and an evaporator temperature of -9°C. They noticed that the performance of the investigated organic DAR systems was very sensitive to the condenser temperature which should not exceed 40°C, and that it required operation with low surrounding temperatures. Rattner and Garimella [13] proposed a fully passive DAR system operating with the working fluid mixture NH_3-NaSCN-He. Detailed design models for the various components of the system were elaborated. They reported COPs in the range 0.11-0.26 at an ambient air temperature of 24ºC, low heat source temperatures of 110-130°C and passive air cooling. These authors reported [14] on the development of a prototype of the theoretically investigated machine, activated by low temperature heat sources(110 – 130°C) and passively air-cooled. The achieved cooling temperatures were suitable for refrigeration (T_{evap}= 6 → 3°C, COP~ 0.06) and air-conditioning (12 → 8°C, COP ~ 0.14; 18 → 14°C, COP ~ 0.17).

The present paper reports on experimental investigations and numerical simulations of a small capacity diffusion-absorption refrigerator in steady-state mode. The machine performance is studied as function of the heat supplied to the generator. In order to follow the temperature evolution at appropriate locations of the refrigerator, it is equipped with ten K-type thermocouples fixed at the inlet and outlet of each of its components and in the refrigerator cabinet. The ambient temperature is also continuously measured. Further, the main heat transfer characteristics of the refrigerator are determined experimentally.

A steady-state simulation model of the machine is then developed using the flow-sheeting software Aspen-Plus and validated basing on the experimental tests. In this context, it is worth to note that diffusion-absorption refrigeration systems were previously modelled with the help of ad hoc programs but never with the Aspen-Plus Platform. Further, a particular approach is here applied, the "Break point" method described by Somers *et al.* [15] to simulate conventional H_2O/LiBr absorption cooling cycles in Aspen-Plus.

2. Working principle

The investigated refrigerator is a small capacity machine designed for hotel rooms with internal dimensions (height x width x depth): 614 mm x 464 mm x 494 mm. It is powered by an electric heater. A 3-D scheme of the refrigerator and its various components are represented in Figures 1 and 2, respectively. The machine is constituted of generator composed of a bubble pump immerged in an externally heated boiler, a rectifier, a condenser, an evaporator, a gas heat exchanger (GHX), an absorber, a solution heat exchanger (SHX), and a liquid tank. Before the unit begins operation, the ammonia rich solution occupies part of the solution tank, bubble pump and boiler. The gas phase is constituted of hydrogen and ammonia and water vapours. When heat is supplied to the generator, the temperature of the ammonia rich solution increases until the boiling point is reached. Ammonia bubbles are then formed. During their ascent in the vertical pump tube, these bubbles lift the ammonia rich solution upward. At the top of the tube, the liquid solution falls down into the boiler under the effect of gravity and the vapours continue their way to the air-cooled rectifier where a partial condensation takes place. Water-rich condensate falls back into the boiler and almost pure ammonia vapour moves on towards the air-cooled condenser where it condensates by releasing heat to ambient air. Uncondensed vapour reaches the solution tank through a pressure equalizer tube. Liquid refrigerant leaving the condenser flows in a separate tube welded to the two-coaxial-pipe gas heat exchanger connecting the absorber and the evaporator. The cold ammonia-hydrogen gas mixture coming from the evaporator flows in the inner tube of this heat exchanger, while the hydrogen exiting the absorber and returning to the evaporator circulates counter currently in the outer annulus. The refrigerant rich gas is introduced at the bottom of the absorber where it rises counter-currently to the ammonia lean solution fed at the top. The ammonia lean solution dissolves the gaseous refrigerant, and the absorption heat is rejected to the ambient. The resulting ammonia rich solution flowing out of the absorber tube ends up in the solution tank. From there it starts to the bubble pump via the solution heat exchanger where it is warmed up by the lean solution exiting the boiler on its way back to the absorber.

3. Experimental procedure and results

As mentioned before, the refrigerator is equipped with 10 K-thermocouples placed at the inlet and outlet of each of its components and connected up via a data acquisition unit (34970A AGILENT) to a computer (Figure 3) where the data is monitored and stored. The locations of the thermocouples on the machine, identified by their ID numbers, are given in Table 1. The ambient temperature T_{amb} as well as the refrigerator cabinet temperature T_{cab} are also continuously measured and registered. Beforehand the thermocouples have been verified by placing them in a calibration ice-water bath. A fluctuation of ±0.5°C of the temperature measured is noticed. The generator electric heater is connected to a power controller in order to operate the machine and to investigate its performance at different energy supply conditions. The experimental tests are carried out by first adjusting the heating power supplied to the generator and then starting the temperature measurements and storing the data at 60s intervals until the refrigerator reaches its steady state regime. Twelve experiments for different energy supply to the generator are performed: 27, 35, 39, 44, 46, 48, 51, 53, 56, 58, 61 and 67 W. Monitoring the temperature profiles helps determining of the minimum power supply needed to ensure the stable functioning of the refrigerator. As illustration, figure 4 shows that a heat supply of 35 W ensures the functioning of the refrigerator but not its stability, while by an energy supply of 39 W (Fig. 5) a stable operation is reached after two and a half hours.

To evaluate the performance of the machine, the coefficient of performance (COP) is used [16]:

$$COP = \frac{\dot{Q}_{evap}}{\dot{Q}_{gen}} \qquad (1)$$

While $\dot{Q}_{gen}$ can be readily determined, the cooling capacity, $\dot{Q}_{evap}$ is indirectly deduced from measured temperatures and appropriate heat transfer models in a many-step procedure. To this purpose, and considering the evaporator, the cooling capacity $\dot{Q}_{evap}$ is written as [16]:

$$\dot{Q}_{evap} = (UA)_{int} \Delta TLM_{evap} \qquad (2)$$

ΔTLM_{evap} is the logarithmic mean temperature difference at cold and hot sides of the evaporator [16]:

$$\Delta TLM_{evap} = \frac{(T_{cab}-T_{out})-(T_{cab}-T_{in})}{\ln\left[\frac{(T_{cab}-T_{out})}{(T_{cab}-T_{in})}\right]} \qquad (3)$$

T_{out}, T_{in} and T_{cab} refer to the measured steady state temperatures of the refrigerant temperature at the inlet and outlet of the evaporator and in the refrigerated cabinet, respectively. $(UA)_{int}$ in equation (2), is the unkown overall heat transfer coefficient of the evaporator.

At steady state, the refrigerated room cabinet energy balance writes $\dot{Q}_{cab} = \dot{Q}_{evap}$, where $\dot{Q}_{cab}$ represents the rate of heat infiltration into the refrigerated room cabinet from outside.

$$\dot{Q}_{cab} = (UA)_{cab}(T_{amb} - T_{int}) \qquad (4)$$

It follows then,

$$(UA)_{cab}(T_{amb} - T_{int}) = (UA)_{int}\Delta TLM_{evap} \qquad (5)$$

or

$$\frac{(UA)_{cab}}{(UA)_{int}} = \frac{\Delta TLM_{evap}}{(T_{amb} - T_{int})} \qquad (6)$$

The last equation indicates that the ratio $\left(\frac{(UA)_{cab}}{(UA)_{int}}\right)$ can be deduced from the corresponding steady state temperature measurements, as shown in figure 6. It is found that $\frac{(UA)_{cab}}{(UA)_{int}} = 1.85$ with an absolute uncertainty of ±0.04.

The value of $(UA)_{int}$ can be evaluated, if $(UA)_{cab}$ is known. The latter is determined by applying a standardized procedure in a separate test. An electric heater in the form of an electric cable ($R = 135\Omega$) is placed in the cabinet and heated. For each power supply to the electric resistance cable the indoor and outdoor temperatures, T_{int} and T_{amb}, of the refrigerator cabinet are measured. At steady state, the power supply to the heating cable $\dot{Q}_{heat}$ equals the total heat losses of the refrigerated room cabinet, *i.e.*

$$\dot{Q}_{heat} = (UA)_{cab}(T_{int} - T_{amb}) \qquad (7)$$

From which it follows:

$$(UA)_{cab} = \frac{\dot{Q}_{heat}}{(T_{int} - T_{amb})} = \frac{\left[\varphi^2/_R\right]}{(T_{int} - T_{amb})} \qquad (8)$$

The experiment is repeated for 7 different values of $\dot{Q}_{heat}$. From the slope of the regression line representing $\left[\varphi^2/_R\right]$ *vs.* $(T_{int} - T_{amb})$, as shown in figure 7 the value of $(UA)_{cab}$

$$(UA)_{cab} = 0.554 \text{ WK}^{-1}$$

is obtained, and finally the value of $(UA)_{int}$ is deduced

$$(UA)_{int} = 0.3 \text{ WK}^{-1}$$

with an absolute uncertainty of ±0.01 WK^{-1}. Once the internal and external heat transfer coefficients determined, the cooling capacity and the COP can be evaluated by applying equations (1) and (2), with an estimated relative uncertainty of 4%. The results are represented in figure 8 depicting the cooling capacity *vs*. rate of heat supply to generator and figure 9, the coefficient of performance. As figure 8 illustrates, by increasing the heat supplied to the generator, from 35 W on, the cooling capacity first increases, reaches a value of 7.3 W for a power supply of 46 W and then remains approximately constant.

From the trend of the COP depicted in figure 9, it is noted that this performance criterion first increases together with the refrigeration capacity for low generator energy supply, reaches a maximum of 0.159, with a power supply of 46 W at a generator temperature of 167°C, and then decreases gradually.

These findings can be interpreted as follows. By increasing the heat supplied to the generator, the flow rates of the pumped solution and of the refrigerant vapour first increase, leading to a progressively larger cooling capacity. A larger flow rate of the pumped solution allows also for the absorption of a greater quantity of refrigerant vapour in the absorber. This explains the initial growth of the cooling capacity and, as a result, the concomitant increase of the coefficient of performance. Further increase of the energy supply does not lead to an improvement of the COP, rather its deterioration, because the cooling capacity comes to a stagnation point as figure 8 shows. Hence, it is not necessary to supply more than 46 W to ensure the functioning of the refrigerator investigated.

4. Aspen-Plus modelling of the diffusion-absorption refrigerator

In this paragraph, steady-state modelling of the commercial diffusion-absorption refrigerator (DAR) is presented using the commercial flow-sheeting software Aspen-Plus [17]. A viable model of the refrigerator, although constituting a simplified conceptual representation of the real machine, should be able to reproduce the actual state at given operating conditions and predict the functioning of the DAR for modified operating conditions.

4.1 Thermodynamic property models

A crucial step in the model development is the selection of a proper method for estimating the thermodynamic properties of the working fluid because of the sensitivity of the simulation results to the properties model. In order to find out the most accurate properties model for the binary ammonia/water fluid mixture, Mansouri *et al*. [18] compared the VLE predictions of nine property methods available in Aspen-Plus in the pressure range from 2 to 25 bar and the temperature range -19 to 220 ºC with the VLE data reported by Mejbri and Bellagi [19]. The Aspen-Plus data regression system facility was also used to fit the interaction parameters of the property models. The VLE predictions of the Peng-Robinson equation of state with the Boston-Mathias alpha function (PR-BM EOS) was found to be the most accurate for the pressure and temperature ranges considered. Figures 10 and 11 depict the comparison of the model predictions with the data at 25 bar. The regressed PR-BM EOS is then selected for the calculation of the thermodynamic properties.

4.2 Refrigerator model

To build a model of the DAR using the ASPAN-PLUS platform, one has first to select the appropriate software element models, referred to as blocks in the ASPEN language, to represent the refrigerator components, and then to combine them to the desired configuration by connecting them through material and eventually energy streams. Table 2 gives the Aspen blocks for the various components of the investigated refrigerator. Condenser and evaporator modelled using a simple heat exchanger, a HEATER block. An ABSORBER block is used for the absorber and a combination of a FLASH and a MIXER for the solution tank. An LNG-HX three-flow exchanger simulates the gas heat exchanger and a two-flow heat exchanger HEATX the solution heat exchanger. Material streams connecting the various components of this machine are identified with their IDs as given in Table 1. It should be noted that no adequate ASPEN blocks are available to represent the complex structure of the combined elements (generator+bubble pump+rectifier). So a simplified model is adopted including four energy and material interconnected blocks. Firstly, the rectifier is modelled using a RECTIFIER block. The generator is represented by a REBOILED STRIPPING block, having as feed the vapour-liquid mixture from the bubble pump and the liquid bottom product of the rectifier. The vapour exiting the top of the generator column feeds the rectifier. The hot solution leaving the boiler of the generator, where the heat needed to drive the refrigerator is supplied, is itself the source of energy for the bubble pump, to which it delivers heat via the heat exchanger BP-PREHX (Fig. 12) before entering the solution heat exchanger. The bubble pump is thus modelled using a combination of FLASH tank and a HEATER block connected with a heat stream.

4.3 Model assumptions and simulation procedure

The main assumptions and data used as inputs for the first simulations are based largely on the experimental steady state test for a generator heating rate 46 W, corresponding to the optimal operating conditions: maximum COP (0.16) and largest cooling capacity (7.3 W). Table 3 summarizes the input data. In this particular test the temperature of liquid refrigerant leaving the condenser is 35°C, and that of the ammonia rich solution at absorber outlet and in the solution tank, 38.4°C. For a generator at about 170°C, the temperature measured at the evaporator inlet is -23°C, and at the outlet -5°C. Further, the usual simulation assumptions are made:

- Saturated liquid solution (ammonia-rich) at outlet of absorber,
- Saturated liquid solution (ammonia-poor) leaving generator,
- Saturated vapour (ammonia quasi pure) at condenser inlet,
- Vapour-liquid equilibrium of water/ammonia mixture at inlet and outlet of evaporator,
- Saturated vapour mixture at top of absorber,
- Saturated liquid leaving condenser,
- Vapour-liquid equilibrium at top of bubble pump.

Two “break points” are integrated into the simulation model to allow for input conditions. The first “break” is inserted at state point 1 (ammonia-rich solution exiting the solution tank), and the second “break” at state point 2 (inert gas flowing in the gas heat exchanger). The identity of streams 1 and 1A on one side and streams 2 and 2A on the other side constitute numerical convergence criteria (Figure 12). The simulations are started using the standard *Sequential* approach: The blocks are solved one-by-one progressively. After convergence and synchronization, the more general *Equation-Oriented* method is used: The large set of nonlinear model equations is solved simultaneously, using an efficient combination of iteration algorithms, and the results of the sequential method to initialize the calculations.

5. Simulation results and discussion

To test the Aspen-Plus model developed for the diffusion-absorption refrigerator, the data measured for a heating power of 46W are used in a first step. The corresponding simulation results are summarized in Table 4. In Table 5, the measured and model calculated temperatures at 9 locations of the machine are compared. A graphical representation of the comparison is depicted in Figure 13. As can be noted, this comparison shows good agreement between model results and the experimental data. Similar concordance is also found when the performance parameters of the DAR are compared (Table 6): The deviations between calculated and measured COP on one hand, and cooling capacity on the other hand, are less than 1%. In Figure 14 the thermodynamic cycle of the DAR machine is plotted on the ammonia/water Dühring diagram for the selected generator heating power. As the whole process is taking place at a uniform pressure of 25 bars, the pressure read from the diagram is significant only in case of saturation and liquid-vapour phase equilibrium.

Consider first the circulation of the aqueous ammonia solution between generator and absorber: The saturated ammonia-lean solution leaves the generator with an ammonia mass fraction of 12.4%, and the ammonia-rich solution exits the absorber with 35% mass fraction. The refrigerant vapours out of the rectifier at a temperature 62ºC become liquid in the condenser and leave it as subcooled condensate at 35ºC. Finally, the cold producing process in the evaporator is taking place under increasing ammonia partial pressure, and hence increasing temperature, from -23°C at the inlet to -5.6ºC at the outlet.

After having successfully tested the developed Aspen-Plus model of the DAR for a heating power of 46W (maximum COP and cooling capacity), it is validated for two larger heating rates ─to avoid fluctuating functioning of the refrigerator for lower rates that is not described by the steady state model─ but otherwise arbitrary chosen values: 56W and 67W. Figures 15 and 16 illustrate the comparison between model-predicted and measured temperatures again at the same 9 locations of the machine as for the 46W case. These figures show that for both new cases the sets of data are in good agreement. Further, the deviations between predictions and measurements of the performance of the refrigerator under the changed operating conditions, as summarized in table 7, are small, less than one per cent. All these results validate the proposed ASPEN-Plus developed, although the generator compartment is only roughly described. More elaborated models for this element of the refrigerator might be conceived and would describe more realistically the behavior of the bubble pump, but as demonstrated in this paper, the simplified model proposed can adequately simulate the steady state behaviour of the small capacity commercial diffusion-absorption refrigerator investigated.

6. Conclusion

A commercial diffusion-absorption refrigerator was tested under different heat input conditions to the generator. The essential characteristics of the refrigerator are determined experimentally, especially the heat exchange capacities of the refrigerated room cabinet and the evaporator. The corresponding values found are $(UA)_{cab} = 0.554\ \mathrm{WK^{-1}}$ and $(UA)_{int} = 0.3\ \mathrm{WK^{-1}}$, respectively. The optimal performance of the refrigerator is reached with an electric power supply of 46 W at a generator temperature of 167°C. A maximum machine COP of 0.159 is attained under these conditions.

An Aspen-Plus model for the diffusion-absorption refrigerator was then developed. A crucial step in the modelling procedure is the selection of an appropriate property model for the working fluid mixture used. It is found from precisions investigations that the Boston-Mathias modified Peng-Robinson equation of state is the most accurate at the pressure and temperature ranges of interest. For the simulations, as well as the operating conditions, a set of assumptions based on the machine experimental tests were introduced as inputs. The calculated temperatures at several locations of the machine for the heating rates 46W, 56W and 67W are found in good agreement with the measured temperatures. The deviations between predicted and measured COP and cooling capacity are about 1%. This indicates that the model developed represents fairly well the functioning of the commercial diffusion-absorption refrigerator working under a steady-state mode.

References

[1] K. Rajasuthan, M. PalPandi, Fabrication and Performance Evaluation of Electrolux Refrigeration System Coupled with IC Engine. Int. J. of Engineering Sciences & Research Technology, 2014, 3 (12), 478-483.

[2] B. C. Von Platen, C. G. Munters, Patent No. 1, 609,34 (United States), 1926.

[3] D.A. Kouremenos, A. Stegou-Sagia, Use of helium instead of hydrogen in inert gas absorption refrigeration. Int. J. of Refrigeration, 1988, 11 (5), 336-341.

[4] J. Chen, K.J. Kim, K.E. Herold, Performance enhancement of a diffusion absorption refrigerator. Int. J. of Refrigeration, 1996, 19 (3), 208-218.

[5] G. Vicatos, Experimental investigation on a three-fluid absorption refrigeration machine. Journal of Process Mechanical Engineering, 2000, 214 (3), 157-172.

[6] A. Zohar, M. Jelinek, A. Levy, I. Borde, Numerical investigation of a diffusion absorption refrigeration cycle. Int. J. of Refrigeration, 2005, 28 (4), 515-525.

[7] N. Ben Ezzine, R. Garma, A. Bellagi, A numerical investigation of a diffusion-absorption refrigeration cycle based on R124-DMAC mixture for solar cooling. Energy, 2010, 35 (5), 1874-1883.

[8] Z. Sayadi, N. Ben Thameur, M. Bourouis, A. Bellagi, Performance optimization of solar driven small-cooled absorption–diffusion chiller working with light hydrocarbons. Energy Conversion and Management, 2013, 74, 299-307.

[9] S. Mazouz, R. Mansouri, A. Bellagi, Experimental and thermodynamic investigation of an ammonia/water diffusion absorption machine. Int. J. of Refrigeration, 2014, 45, 83-91.

[10] K.G. Narayankhedkar, M. Prakash Maiya, Investigations on triple fluid vapour absorption refrigerator. Int. J. of Refrigeration, 1985, 8 (6), 335-342.

[11] A. Zohar, M. Jelinek, A. Levy, I. Borde, The influence of diffusion absorption refrigeration cycle configuration on the performance. Applied Thermal Engineering, 2007, 27 (13), 2213-2219.

[12] A. Zohar, M. Jelinek, A. Levy, I. Borde, Performance of diffusion absorption refrigeration cycle with organic working fluids. Int. J. of Refrigeration, 2009, 32 (6), 1241-1246.

[13] A.S. Rattner, S. Garimella. Low-source-temperature diffusion absorption refrigeration. PartI: Modeling and cycle analysis. International Journal of Refrigeration, 2016, 65, 287-311.

[14] A.S. Rattner, S. Garimella. Low-source-temperature diffusion absorption refrigeration. Part II: Experiments and model assessment. International Journal of Refrigeration, 2016, 65, 312-329.

[15] C. Somers, A. Mortazavi, Y. Hwang, R. Radermacher, P. Rodgers, S. Al-Hashimi, Modeling water/lithium bromide absorption chillers in Aspen Plus. Applied Energy, 2011, 88 (11), 4197-4205.

[16] Keith E. Herold, Reinhard Radermacher, Sanford A. Klein, Absorption Chillers and Heat Pumps. CRC Press, Inc, 1996.

[17] Aspen Plus. Version 7.3.0.13 (25.0.4987), 2009. Aspen Technology, Inc., Ten Canal Park, Cambridge, MA, USA,www.aspentech.com.

[18] R. Mansouri, I. Boukholda, M. Bourouis, A. Bellagi, Modelling and testing the performance of a commercial ammonia/water absorption chiller using Aspen-Plus platform. Energy, 2015, 93, 2374-2383.

[19] K. Mejbri, A. Bellagi, Modelling of thermodynamic properties of the water-ammonia by three different approaches. Int. J. of Refrigeration, 2006, 29 (2), 211-218.

[20] R. Best, W. Rivera, A review of thermal cooling systems. Applied Thermal Engineering, 2015, 75, 1162-1175.

[21] W. Wu, B. Wang, W. Shi, X. Li, An overview of ammonia-based absorption chillers and heat pumps. Renewable and Sustainable Energy Reviews, 2014, 31, 681-707.

[22] J.L. Rodríguez-Muñoz, J.M. Belman-Flores, Review of diffusion-absorption refrigeration technologies. Renewable and Sustainable Energy Reviews, 2014, 30, 145-153.

[23] K.J. Chua, S.K. Chou, W.M. Yang, J. Yan, Achieving better energy-efficient air conditioning- A review of technologies and strategies. Applied Energy, 2013, 104, 87-104.

Table captions

Table 1. Locations of the thermocouples

Table 2. Machine components and their Aspen-Plus models (Figure.33)

Table 3. Data input for simulation (operation under optimal conditions)

Table 4. Simulation results of the diffusion-absorption refrigerator using the Aspen-Plus model for $\dot{Q}_{gen} = 46$ W

Table 5. Measured and model predicted temperatures for $\dot{Q}_{gen} = 46$ W

Table 6. Calculated and experimental performance parameters of the diffusion-absorption refrigerator

Table 1. Locations of the thermocouples

Location	Thermocouple and stream ID
Generator gas outlet	101
Condenser outlet	103
Gas heat exchanger outlet	104
Evaporator outlet	105
Interior refrigerator	106
Absorber gas outlet	107
Absorber liquid outlet	108
Evaporator inlet	109
Liquid tank	110
Liquid generator outlet	112
Ambient air	115

Table 2. Machine components and their Aspen-Plus models (Fig.12)

Component (Name in Fig.12)	**Aspen Block**
Condenser (CNDNSER)	HEATER
Evaporator (EVAP)	HEATER + MIXER
Absorber (ABSORBER)	ABSORBER
Solution heat exchanger Two-flow heat exchanger (SOL-HX)	HEATX
Generator (GEN)	REBOILED STRIPING BLOCK (STRIP1)
Rectifier (RECT)	RECTIFIER
Refrigerant tank (TANK)	FLASH + MIXER
Gas heat exchanger Three-flow heat exchanger (GGHX)	LNG-HX
Bubble pump	FLASH + HEATER

Table 3. Data input for 1. case simulation ($\dot{Q}_{gen} = 46$ W, $P = 25$bar)

Block	Input
Solution heat exchanger	Ammonia-rich solution outlet temperature, 110°C **State point 1** ○ Temperature, 38.4°C ○ Total mass flow, 0.190 kg/h ○ NH_3 mass fraction, 0.35
Generator	Heat duty, 46 W
Condenser	Outlet temperature, 35°C
Gas heat exchanger	ΔT stream 103: -30 °C ΔT stream 2: -22 °C **State point 2** ○ Temperature, 27.5°C ○ Total mass flow, 0.019 kg/h ○ H_2 mass fraction, 0.907
Evaporator	Outlet temperature, -5.6 °C
Absorber	Outlet temperature, 38.4°C
Solution tank	Temperature, 38.4°C

Table 4. Simulation results for $\dot{Q}_{gen} = 46$ W

(System pressure, 25bar)

State point	Connection	*T* (°C)	Vapour fraction	Mass flow rate (kg/h)	NH_3 mass fraction (%)	H_2 mass fraction (%)
1A	TANK / SOL-HX	38.4	0	0.190	35.0	0
2A	GGHX-IN / GGHX	27.5	1	0.019	8.3	90.7
101	GEN / RECT	122.4	1	0.091	94.5	0
103	CNDNSER /GGHX	35.0	0	0.049	99.9	0
109	EVAP-IN / EVAP	-23.0	0.798	0.068	74.6	25.1
105	EVAP / GGHX	-5.6	0.873	0.068	74.6	25.1
104	GGHX /ABSORBER	25.3	0.997	0.068	74.6	25.1
COLD-LEAN	SOL-HX / ABSORBER	71.1	0	0.141	12.4	0
108	ABSORBER / TANK	35.8	0	0.190	35.0	0
110-1A	TANK / SOL-HX	38.4	0	0.190	35.0	0
112	BP-PREHX / SOL-HX	167.0	0	0.141	12.4	0
TO-BP	SOL-HX / BBL-PUMP	110.0	0	0.190	35.0	0
HOT-LEAN	GEN / BP-PREHX	191.3	0	0.141	12.4	0
R-LIQ	RECT / GEN	64.1	0	0.042	88.1	0

Table 5. Measured and model predicted temperatures for $\dot{Q}_{gen} = 46$ W

Thermocouple and stream ID	Measured Temp. (°C)	Simulated Temp. (°C)
101	132.1	122.4
103	35.0	35.0
104	24.7	25.3
105	-5.6	-5.6
107	27.5	27.5
108	37.1	35.8
109	-20.5	-23.0
110	38.4	38.4
112	166.3	167

Table 6. Calculated and experimental performance parameters of the diffusion-absorption refrigerator

Parameter	Experimental	Calculated
$\dot{Q}_{gen}$ (W)	46	46
$\dot{Q}_{evap}$ (W)	7.29	7.27
COP	0.159	0.158

Table 7. Calculated and experimental performance parameters of the diffusion-absorption refrigerator for $\dot{Q}_{gen}$= 56W and for $\dot{Q}_{gen}$= 67W

Parameter	Experimental	Calculated	Experimental	Calculated
$\dot{Q}_{gen}$ (W)	56	56	67	67
$\dot{Q}_{evap}$ (W)	7.30	7.25	7.50	7.42
COP	0.130	0.129	0.111	0.110

Figure captions

Figure 1. Schematic view of the diffusion-absorption refrigerator

Figure 2. 3D-Schematic representation of the main components of the diffusion-absorption refrigerator

Figure 3. Experimental set-up

Figure 4. Temperature evolution for generator heat supply of $\dot{Q}_{gen}$= 35W.

Figure 5. Temperature evolution for generator heat supply of $\dot{Q}_{gen}$= 39W.

Figure 6. $(T_{amb} - T_{int})$ *vs.* ΔTLM_{evap}

Figure 7. $\left[\varphi^2/_R\right]$ *vs.* $(T_{int} - T_{amb})$

Figure 8. Cooling capacity *vs*. generator power supply

Figure 9. COP *vs*. generator power supply

Figure 10. *T*-*x*-*y* VLE diagram at *P* = 25 bar for ammonia/water fluid mixture

Figure11. *T*-*x*-*y* VLE diagram at *P* = 25 bar for ammonia/water fluid mixture with regressed PR-BM parameter

Figure 12. Aspen-Plus model of the diffusion-absorption refrigerator

Figure13. Comparison between calculated and experimental temperatures for $\dot{Q}_{gen}$= 46W

Figure 14. Diffusion-absorption refrigeration cycle on Dühring diagram

Figure 15. Comparison between model predictions and experimental temperatures for $\dot{Q}_{gen}$= 56W

Figure 16. Comparison between model predictions and experimental temperatures for $\dot{Q}_{gen}$= 67W

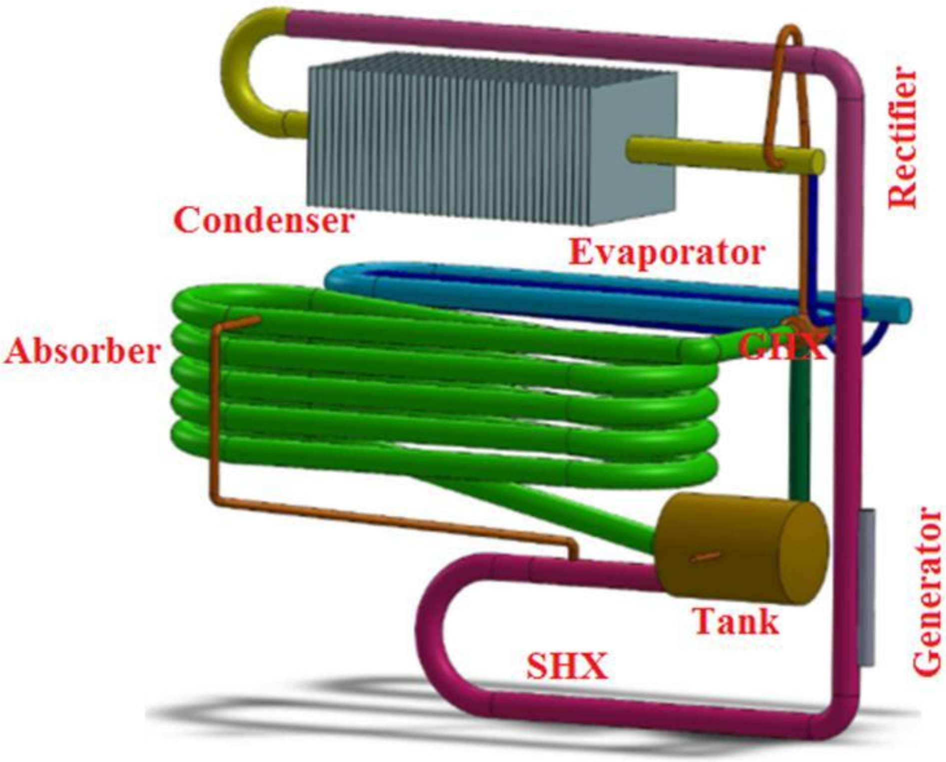

Figure 1. Schematic view of the diffusion-absorption refrigerator

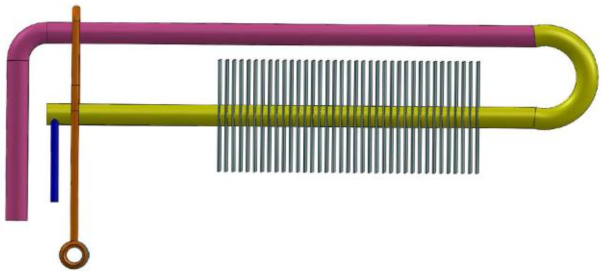

(a) Condenser + Rectifier + Gas Heat Exchanger

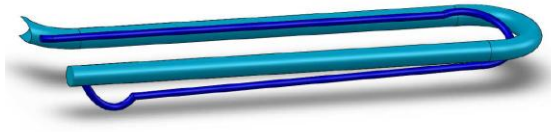

(b) Evaporator

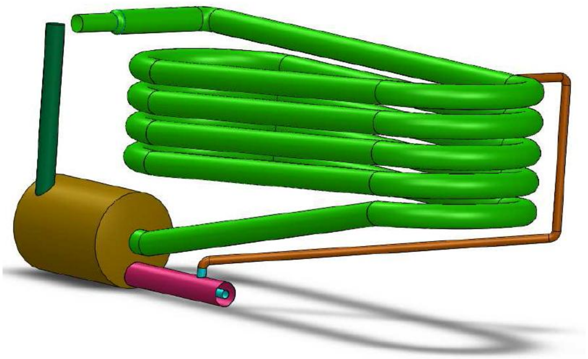

(c) Absorber + Solution tank

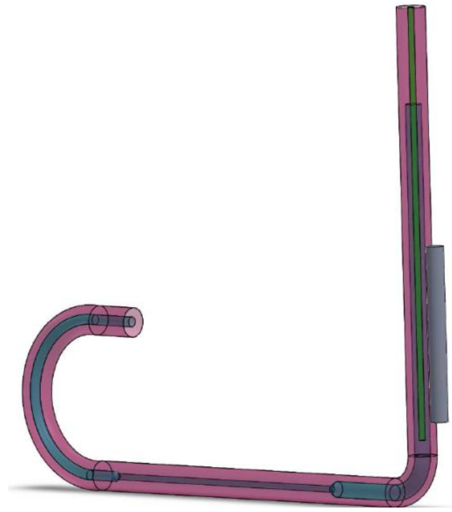

(d) Generator + Bubble Pump + Solution Heat Exchanger

Fig. 2. 3D-Schematic representation of the main components of the diffusion-absorption refrigerator

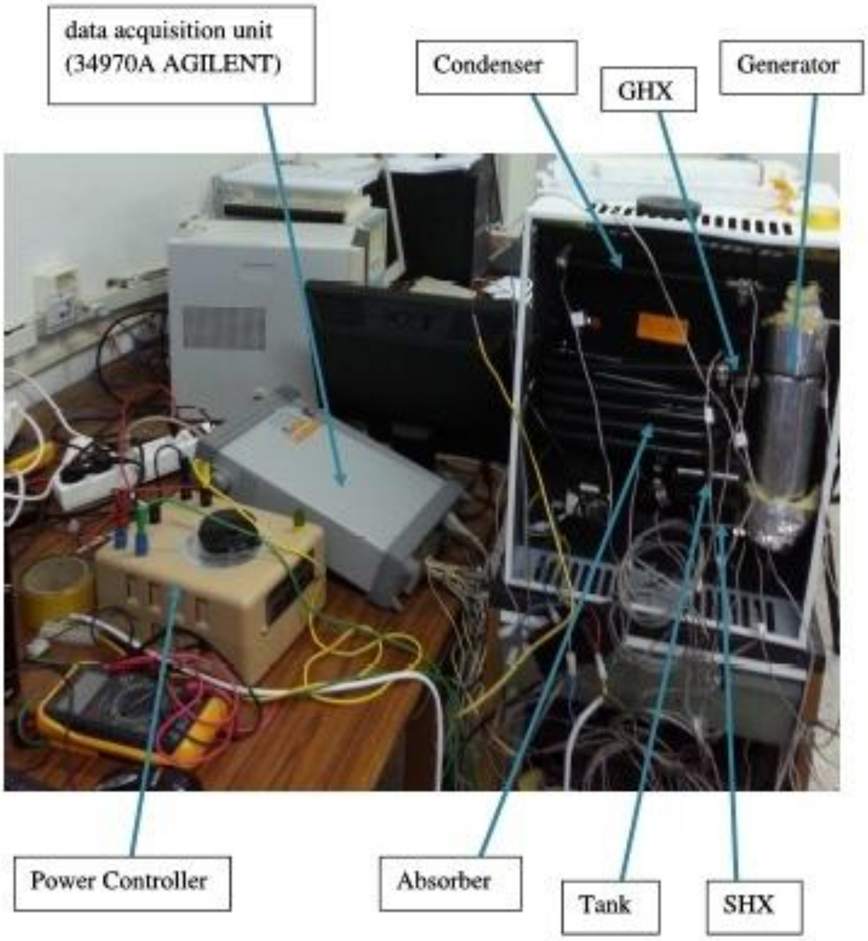

Figure 3. Experimental set-up

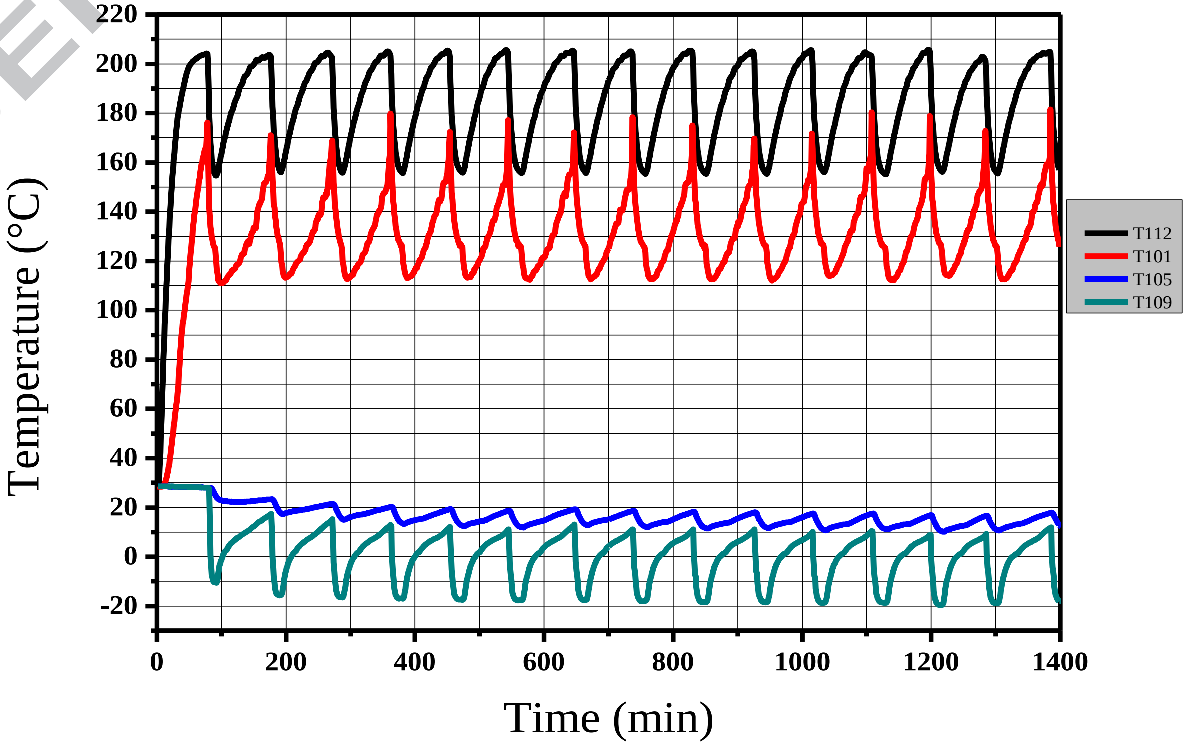

Figure 4. Temperature evolution for generator heat supply of $\dot{Q}_{gen}$= 35W.

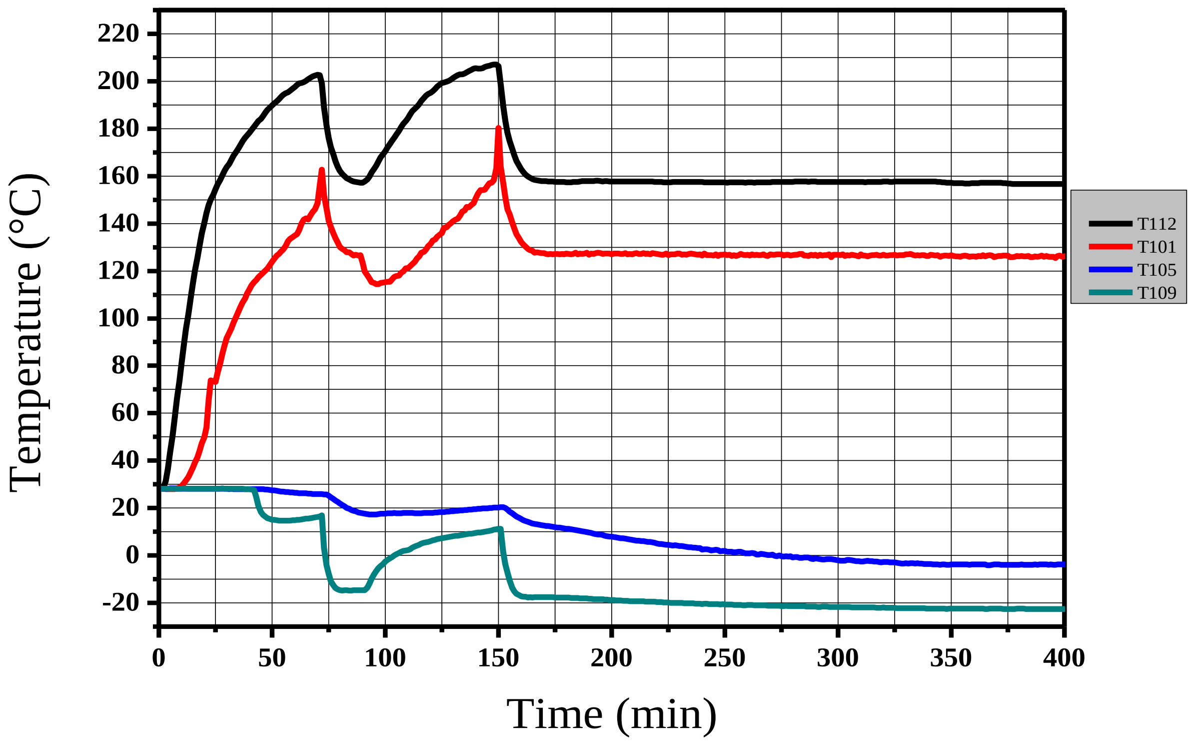

Figure 5. Temperature evolution for generator heat supply of $\dot{Q}_{gen}$= 39W.

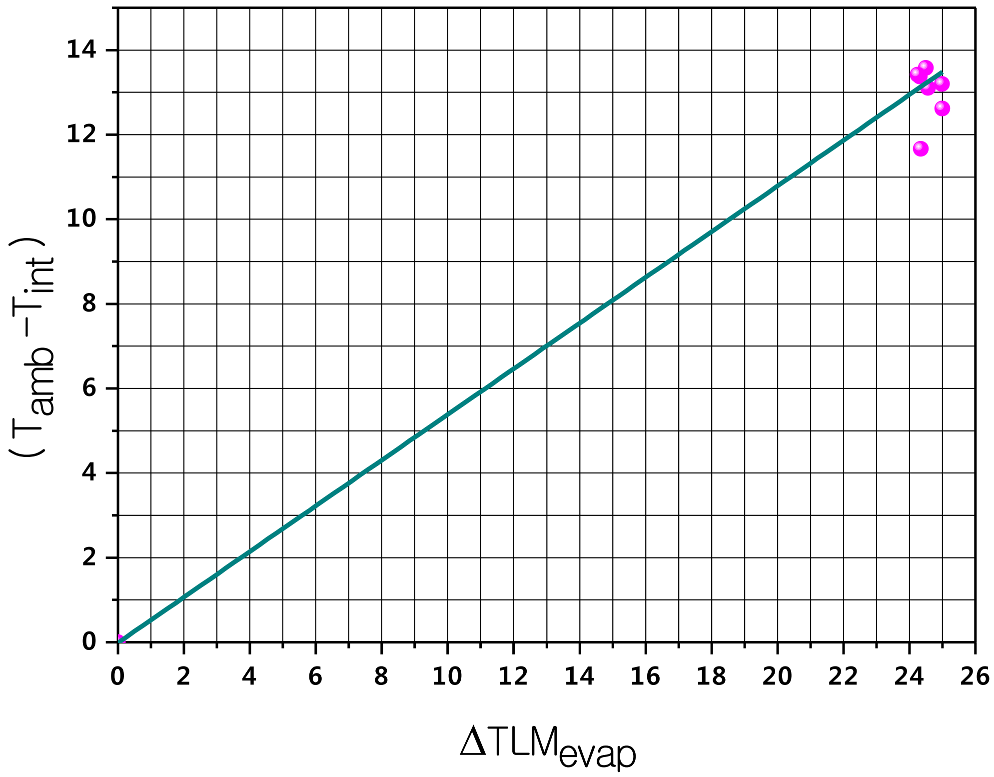

Figure 6. $(T_{amb} - T_{int})$ vs. ΔTLM_{evap}

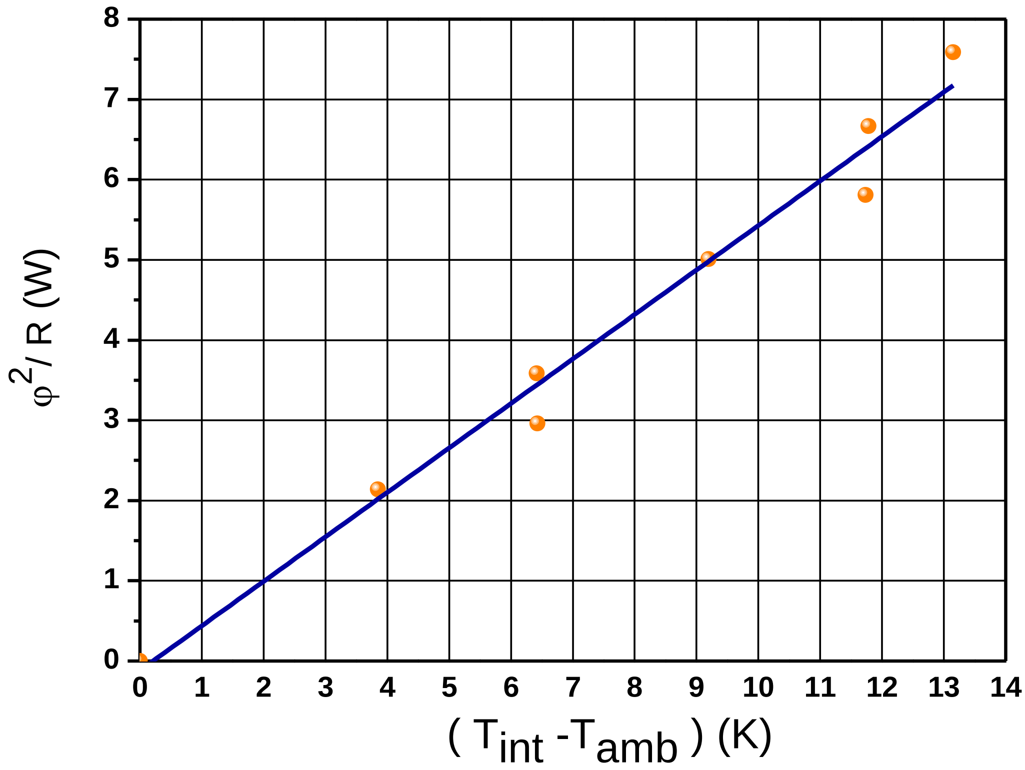

Figure 7. $\left[\varphi^2/_R\right]$ vs.$(T_{int} - T_{amb})$

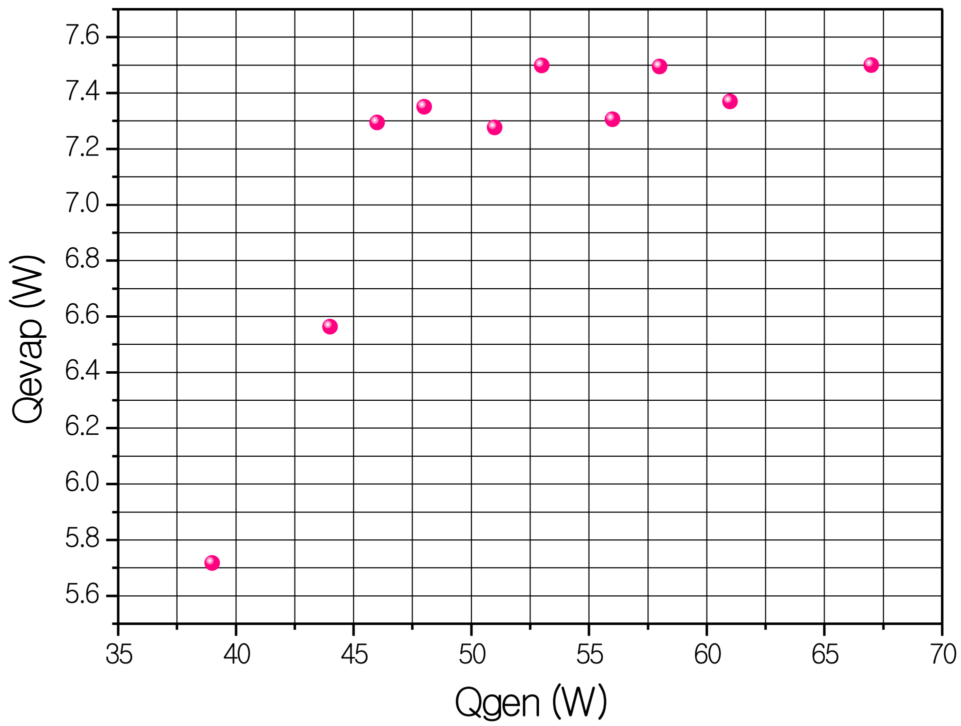

Figure 8. Cooling capacity *vs*. generator power supply

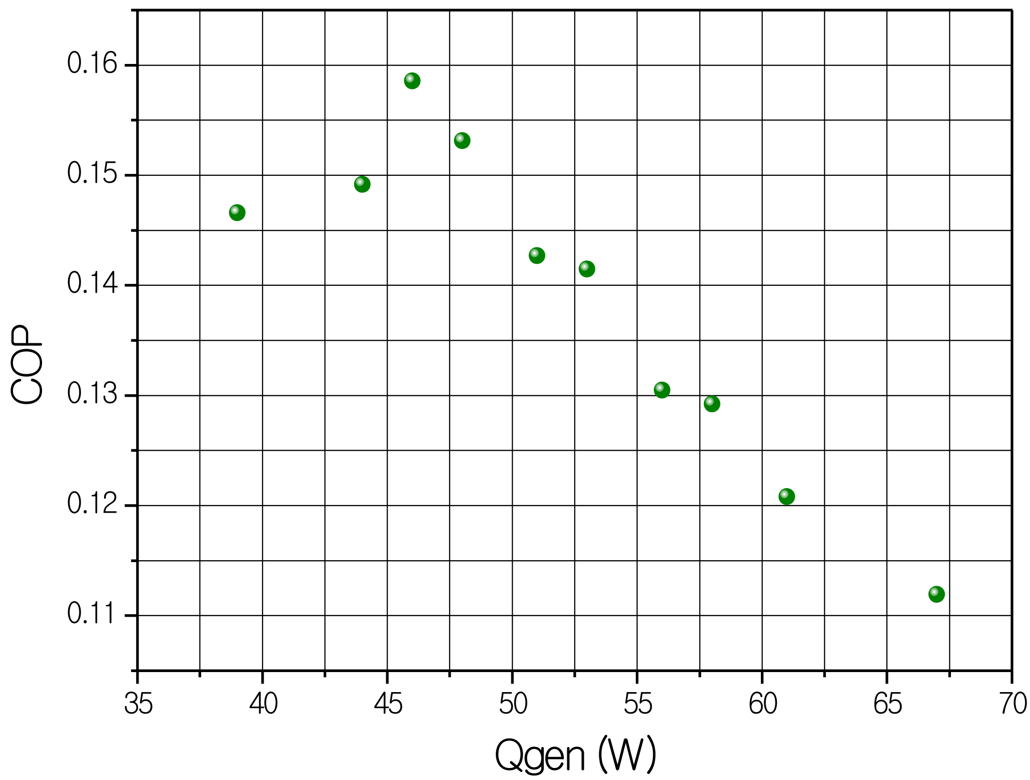

Figure 9. COP *vs*. generator power supply

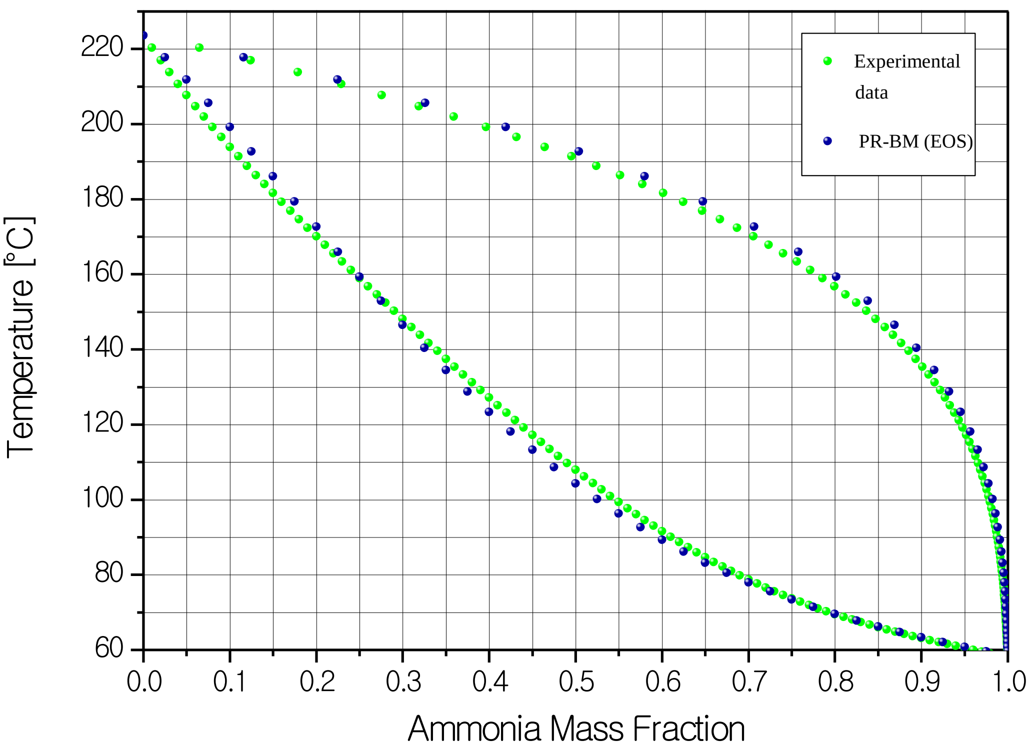

Figure 10. *T*-*x*-*y* VLE diagram at *P* = 25 bar for ammonia/water fluid mixture

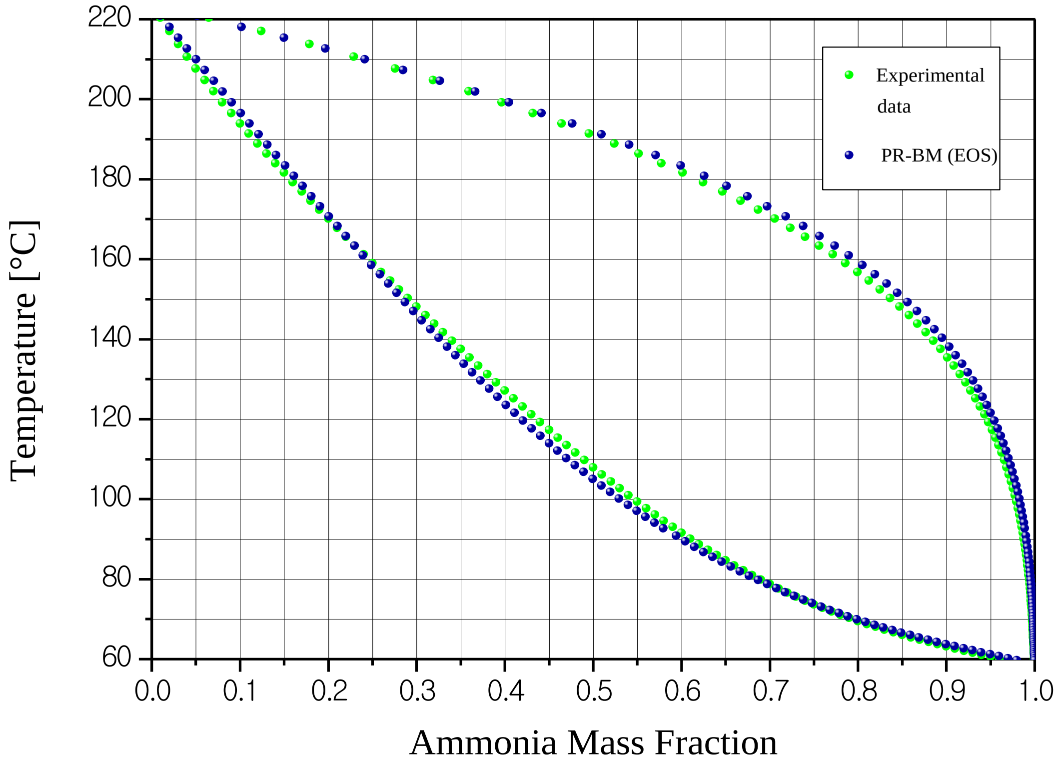

Figure11. *T*-*x*-*y* VLE diagram at *P* = 25 bar for ammonia/water fluid mixture with regressed PR-BM parameter

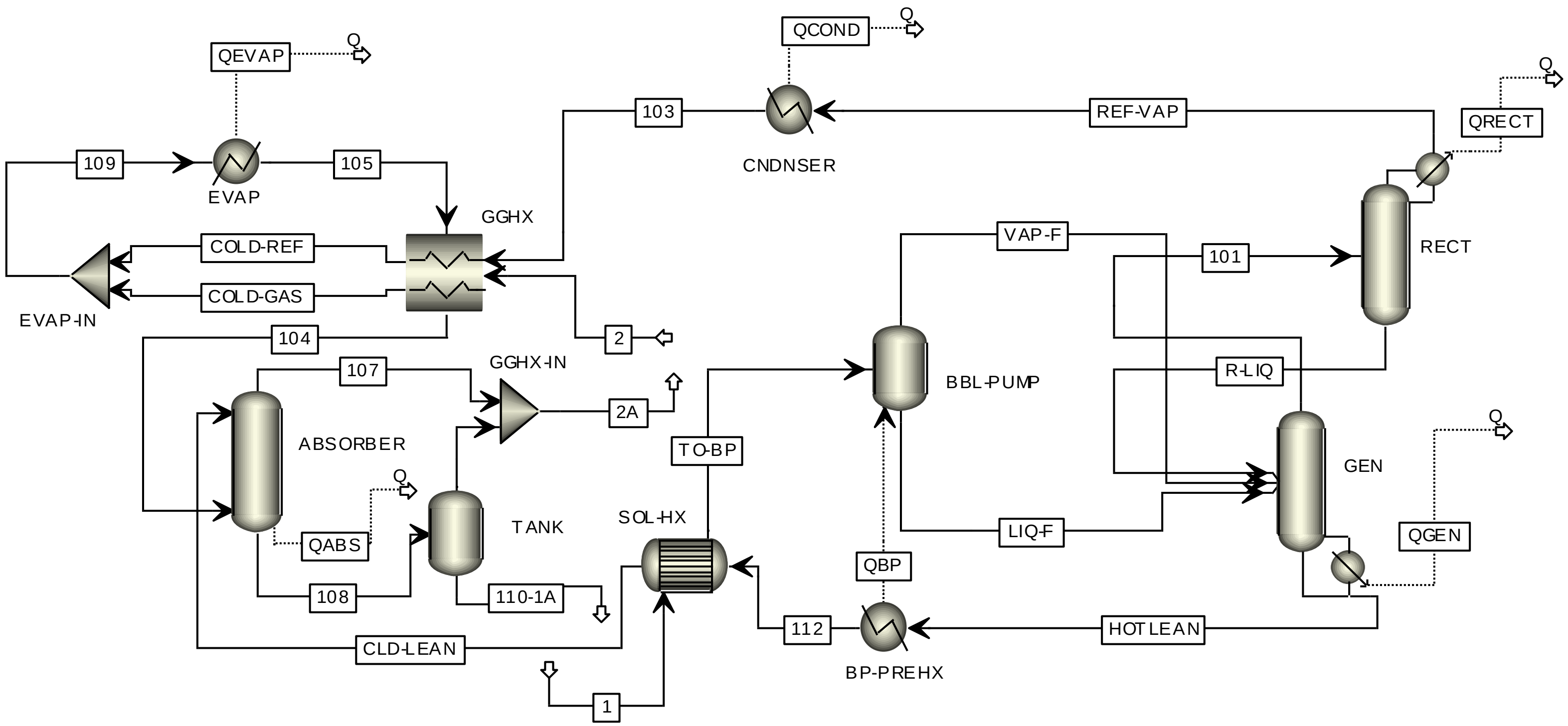

1

2 Figure12. Aspen-Plus model of the diffusion-absorption refrigerator

3

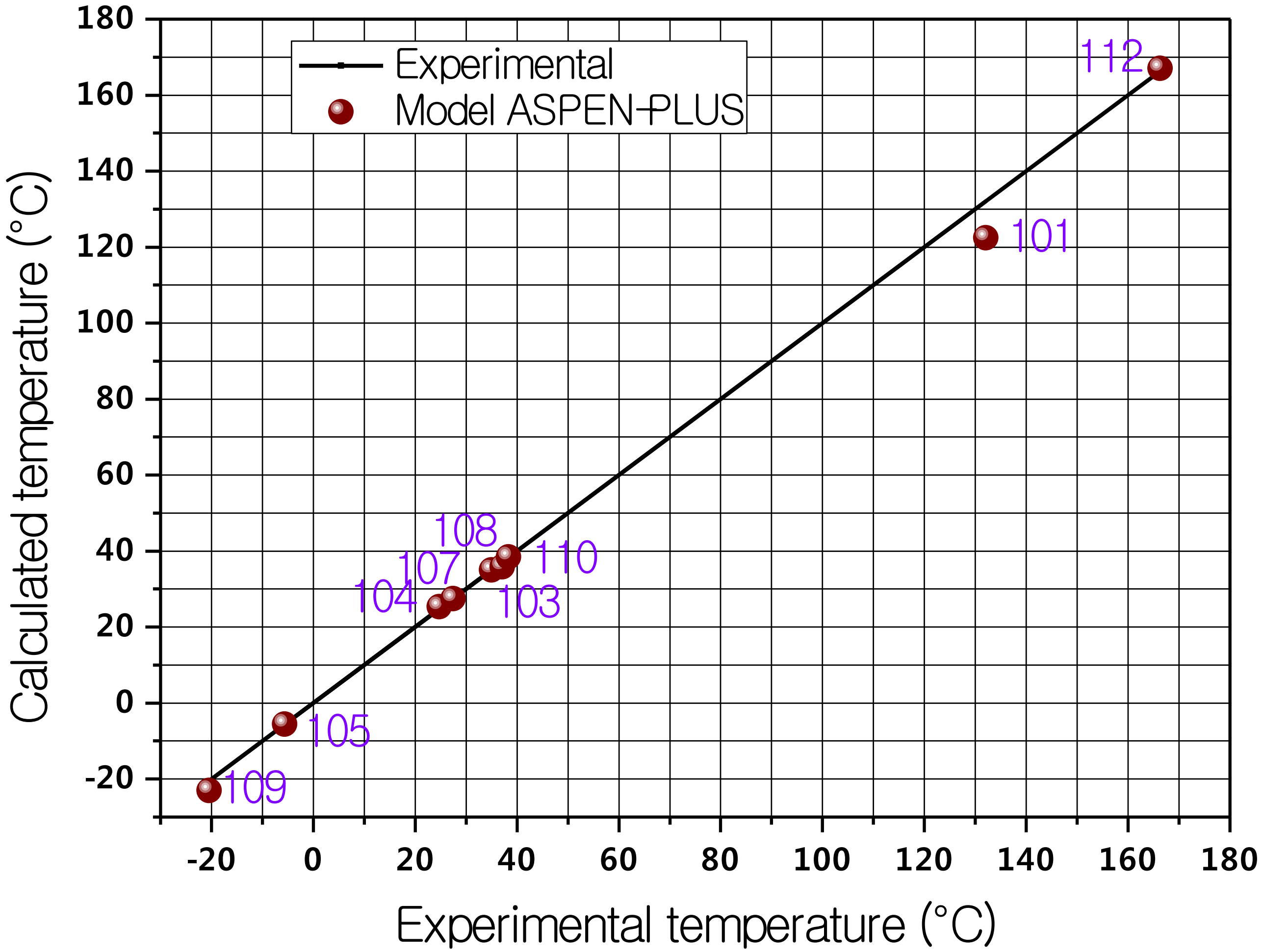

4

5

6 Figure13. Comparison between calculated and experimental temperatures for $\dot{Q}_{gen}$ = 46W

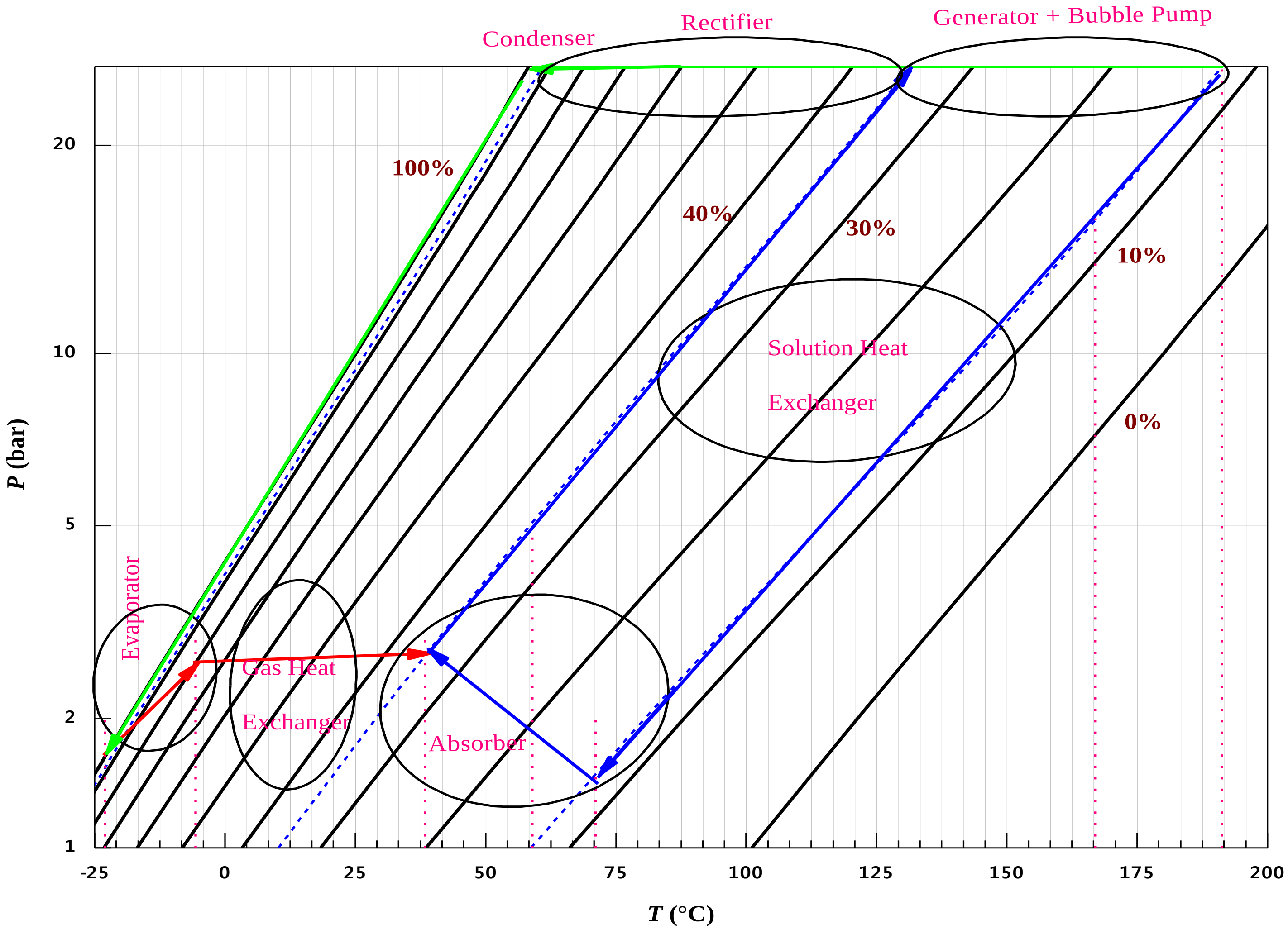

Condenser
Rectifier
Generator + Bubble Pump
100%
40%
30%
10%
0%
Solution Heat
Exchanger
Evaporator
Gas Heat
Exchanger
Absorber
20
10
5
2
1
P (bar)
-25
0
25
50
75
100
125
150
175
200
T (°C)

Figure14. Diffusion-absorption refrigeration cycle on Dühring diagram

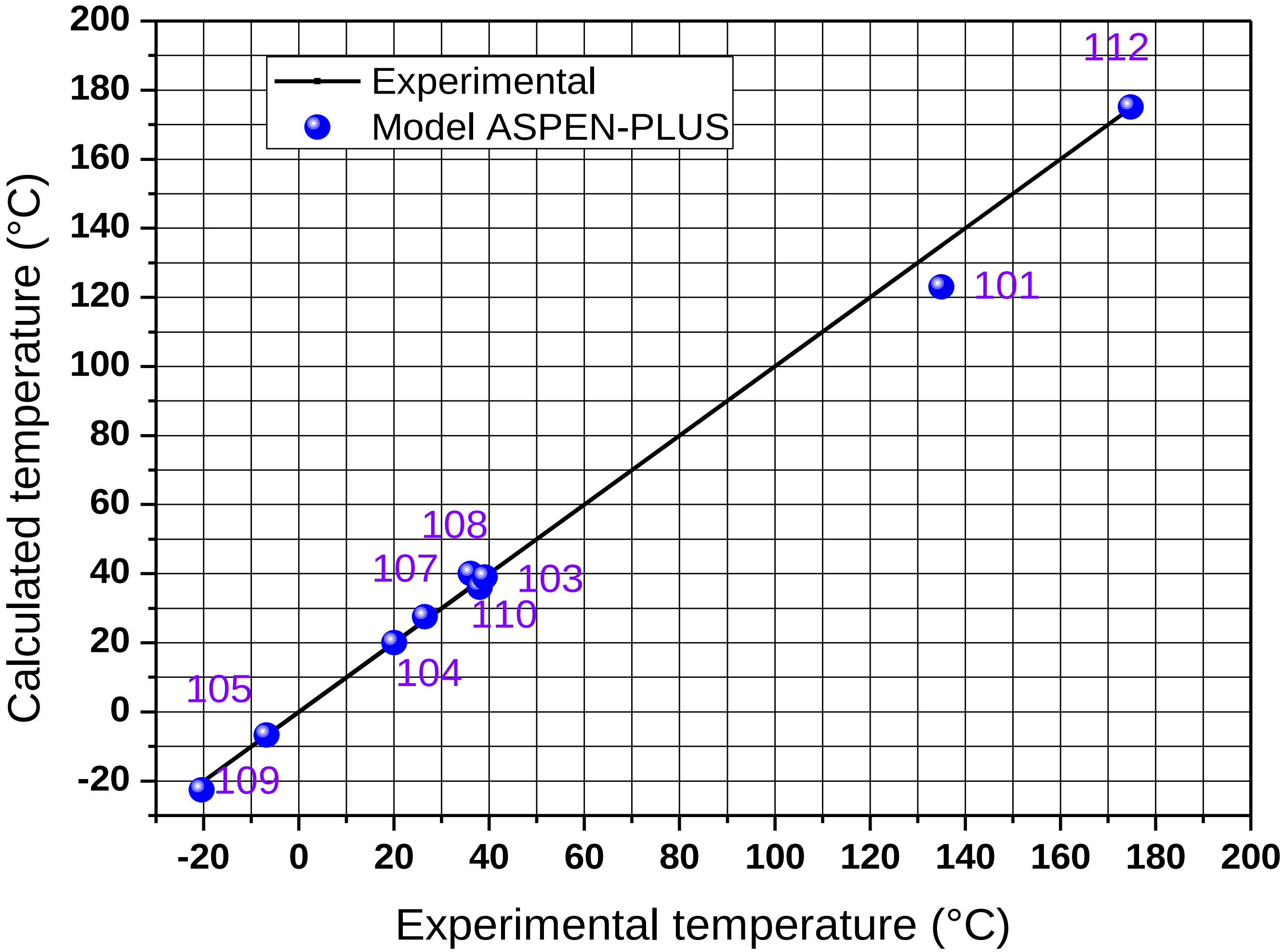

Figure15. Comparison between model predictions and experimental temperatures for $\dot{Q}_{gen}$= 56W

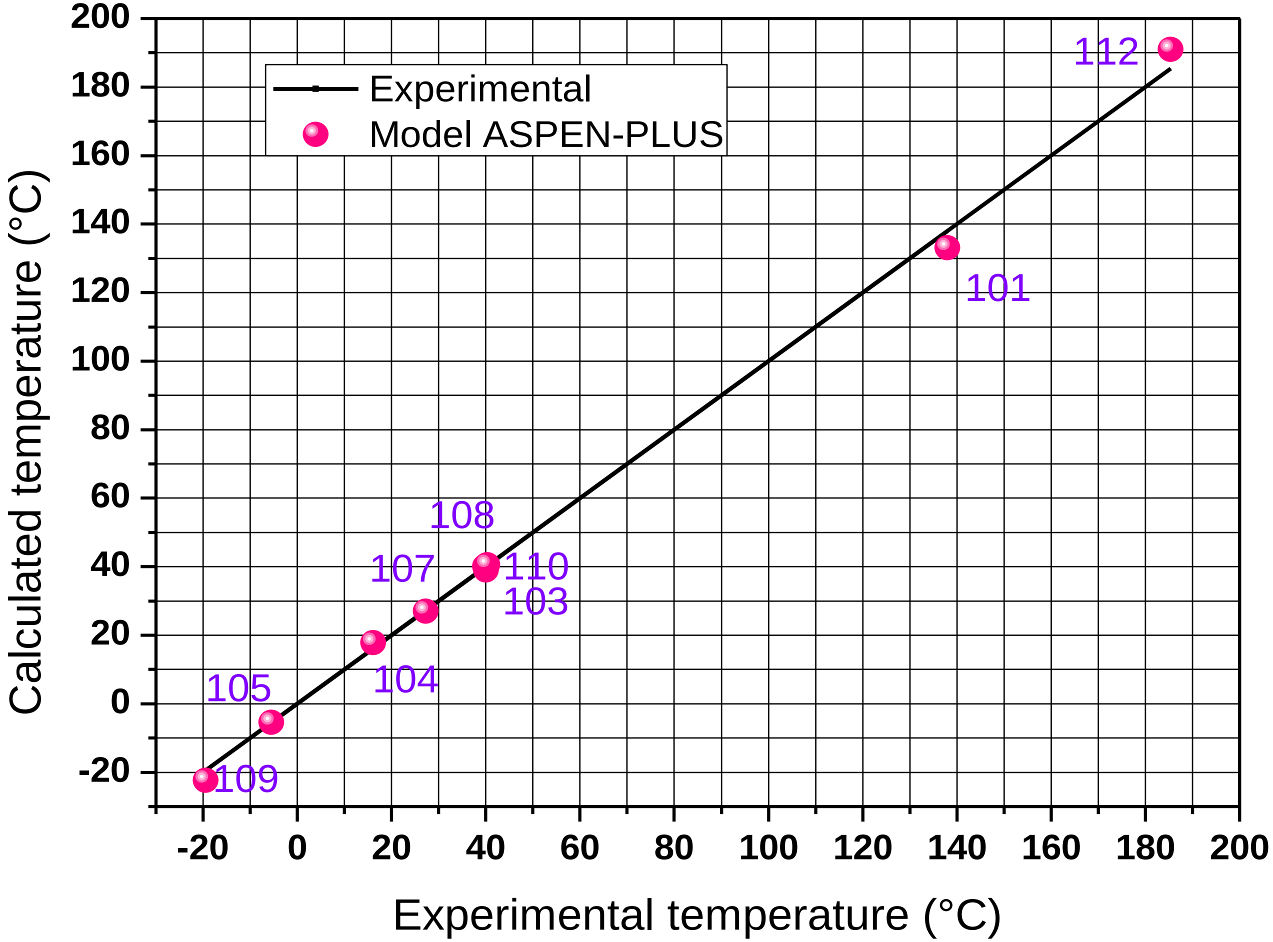

Figure16. Comparison between model predictions and experimental temperatures for $\dot{Q}_{gen}$= 67W